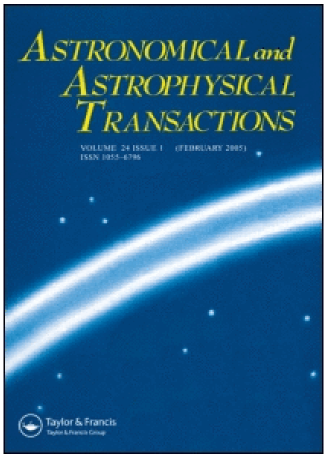

Astronomical & Astrophysical Transactions
The Journal of the Eurasian Astronomical Society
Publication details, including instructions for authors and subscription information:
http://www.informaworld.com/smpp/title~content=t713453505

Simulation of the collapse of a rotating gas cloud on triangular reconstructing lagrangian grid

N. V. Ardeljan [a]; G. S. Bisnovatyi-kogan [b]; K. V. Kosmachevskii [a]; S. G. Moiseenko [ab]

[a] Department of Computational Mathematics and Cybernetics, Moscow State University, Moscow, Russia
[b] Space Research Institute, Moscow, Russia

Online Publication Date: 01 July 1996
To cite this Article: Ardeljan, N. V., Bisnovatyi-kogan, G. S., Kosmachevskii, K. V. and Moiseenko, S. G. (1996) 'Simulation of the collapse of a rotating gas cloud on triangular reconstructing lagrangian grid', Astronomical & Astrophysical Transactions, 10:4, 341 - 355
To link to this article: DOI: 10.1080/10556799608205451
URL: http://dx.doi.org/10.1080/10556799608205451

Astronomical and Astrophysical Transactions, 1996, Vol. 10, pp. 341–355
Reprints available directly from the publisher
Photocopying permitted by license only

SIMULATION OF THE COLLAPSE OF A ROTATING GAS CLOUD ON TRIANGULAR RECONSTRUCTING LAGRANGIAN GRID

N. V. ARDELJAN[1], G. S. BISNOVATYI-KOGAN[2], K. V. KOSMACHEVSKII[1], and S. G. MOISEENKO[1,2]

[1] *Department of Computational Mathematics and Cybernetics, Moscow State University, Vorobjevy gory, Moscow B-234 119899, Russia*
[2] *Space Research Institute, Profsoyuznaya 84/32, Moscow 117810, Russia*

(Received October 19, 1994)

In this paper we consider 2D numerical simulation of the gravitational collapse of a rotating gas cloud. Calculations were made using numerical scheme in Lagrangian variables on triangular irregular grid with grid reconstructing procedure. The most important result is that at the end of calculations flattened disk-shaped body is formed. Previous numerical simulations which have been made in Eulerian coordinate system for the same initial conditions led to ring-shaped body formation. Our results qualitatively coincide with simulations made in Lagrangian coordinates by other authors.

INTRODUCTION

The choice and justification of numerical methods for 2D calculations for rotating bodies are very important. Astrophysical collapse problems are characterized by strong change of density and temperature during a short period of time and the necessity to include gravitation. Under such conditions, the known 2D hydrodynamical methods of calculations have been modified for inclusion of gravitation and possibility for steep gradients appearance (see, e.g. Larson, 1972; Bodenheimer & Tscharnuter, 1979; Kamiya, 1977; Black & Bodenheimer, 1976; Boss, 1980; Norman *et al.*, 1980; Ardeljan *et al.*, 1987a). The group of Eulerian schemes shows that collapse results in the formation of a torus or a ring-like structure (Black & Bodenheimer, 1976; Boss, 1980), whereas Langrangian methods lead to the formation of a disk-like figure (Kamiya, 1977).

Norman *et al.* (1980) used both methods (Lagrangian and Eulerian) to simulate collapse of a rotating core. Their improved Eulerian code, free of artificial inward angular momentum diffusion led to disk formation, as well as their Lagrangian code. Norman *et al.* (1980) mentioned shortcomings of their Lagrangian code which made it less powerful then their Eulerian code:

(1) poor accuracy of difference operators in distorted parts of the grid;
(2) complicated solution of the Poisson equation;
(3) expensive calculations.

The last two shortcomings become not so important when using powerful computers. In our calculations we used about 12000 triangular sells, instead of 400 zones of Norman *et al.* (1980). That gave far better accuracy. The most important is the first point connected with grid distortion and loss of accuracy. The main advantage of our method in comparison with other Lagrangian ones, used in astrophysics till now, is using the procedure of grid restructuring that allows to overcome the grid distortion problem and carry on calculations through large compressions and expansions stages without loss of accuracy. This becomes possible because the adoption of a triangular grid allows to formalize the procedure of grid reconstruction and corresponding redetermination of cell grid functions, and to make it available in automatic regime in the process of calculations.

Kamiya (1977) used a Lagrangian difference method for hydrodynamics and finite element approach for calculation of gravitational potential and demonstrated that a ring-like structure is formed when numerical (unphysical) angular momentum transfer toward the rotational axis takes place. This kind of numerical angular momentum transfer occurred in the calculations mentioned above made using earlier Eulerian difference schemes.

Numerical methods for simulations of the collapse of rapidly rotating cool gas cloud must satisfy the following requirements:

- absence of artificial transfer of angular momentum;
- using of free boundary conditions at the outer boundary of the cloud when the boundary surface moves to a large extent.

A cloud becomes flattened at a developed stage of its collapse, and methods must provide sufficient accuracy when almost 90% of matter is in a thin layer ($\sim 0.04R_0$ where R_0 is the initial radius of the cloud) near the equatorial plane. That requires either strongly nonuniform grid, concentrated near the equatorial plane, or an adaptive Eulerian grid. The Lagrangian grid becomes significantly distorted during collapse, so restructing is necessary in the process of computation. The necessity of rezoning the grid was pointed out earlier by Kamiya (1977), who started calculation of the collapse with the Lagrangian method, but did not extend it to the developed stage because of grid distortion.

Lagrangian numerical schemes are free of the artificial transfer of angular momentum, and free boundary conditions at the outer boundary of the cloud can be satisfied exactly. As pointed out by Normal *et al.* (1980), cells become flattened near the equatorial plane soon after the start of the collapse, thus significantly reducing the accuracy of calculations. They suggested the grid to be refined near the center of the cloud. Our calculations show that the grid should be refined not only in the central part of the cloud but also near the equatorial plane.

Ardeljan *et al.* (1987a) solved this problem using an implicit conservative difference scheme on a Lagrangian triangular grid, whose stability was proved in several mathematical papers (Ardeljan & Chernigovskii, 1984; Ardeljan *et al.*, 1987c). The severe restriction on the number of grid points and the absence of the grid restructuring procedure urged the termination of the calculation of the variant with rapid rotation soon after reflection of the shock at the equatorial plane. The conclusion about the formation of a disk-like structure obtained in this paper was doubted by Boss (1989), who stated that ring formation occurs at later stages. Our present results have shown that the feeble ring-like structure develops transiently after the appearance of the shock wave. It disappears soon during an expansion phase and never reappears.

The use of a 2D code to simulate the collapse of a rapidly rotating cloud cannot describe the devélopment of the three-axial instability which occurs at large ratios of rotational energy to gravitational one (Ostriker & Peebles, 1973). Nevertheless, the development time of the tree-axial instability exceeds the free-fall hydrodynamical time (Chandrasekhar, 1973; Miyama, 1992). Therefore, we expect that the dynamics stage of collapse calculated here can be described by a 2D code rather adequately.

In this paper, the 2D problem of the collapse of a rapidly rotating gas cloud was calculated using the Lagrangian method with a triangular grid for which the following improvements have been made, compared to the method used by Ardeljan *et al.* (1987a):

(1) The grid restructuring procedure developed by Ardeljan *et al.* (1985) was introduced. It allowed us to follow the collapse of the cloud throughout formation of shock wave up to the phase of secondary compression which takes place at much higher entropy. Ardeljan *et al.* (1987a) terminated this version of simulations just before the moment of the shock formation because grid distortions in the inner parts of the cloud prevented further calculations leading to a loss of accuracy with possible overlapping of the grid. Nevertheless, the conclusion of Ardeljan *et al.* (1987a) concerning formation of a disk structure is confirmed here.

(2) Relative accuracy of calculations in the region surrounding rotation axis is not sufficient in first-order methods for the solution of the Dirichlet problem for the Poisson equation. The radial component of the gravitational force near the z-axis is small $F_r \sim r$, and it is comparable with numerical error at small r. The ignorance of these facts by Ardeljan *et al.* (1987a) resulted in false anisotropy of gravitational force near the z-axis and formation of an artificial "dumbbell" structure in the central part of the cloud.

In our simulations, the region close to the rotation axis is handled separately in order to minimize numerical errors. As a result, gravitational force was computed at better accuracy near the center, and, no artificial structure ("dumbbell") emerged and smooth density behavior was obtained.

(3) Owing to better computing facilities (CONVEX C220 instead of BESM-6), the number of grid cells was approximately 12000 compared with only 396 used by Ardeljan *et al.* (1987a). This quantitative modification has led to a qualitative improvement: elimination of numerical errors near the axis, resolved shock front and determination of the amount of matter (~5%) drawn away by the shock.

The method developed here can be applied to the problem of core collapse, to the formation of rapidly rotating neutron stars (Ardeljan *et al.*, 1987b) and to magnetorotational supernova explosions (Bisnovatyi–Kogan, 1970).

1 BASIC EQUATIONS; INITIAL AND BOUNDARY CONDITIONS

Hydrodynamical equations with gravity for modelling unsteady processes in rotating gaseous bodies are:

$$\frac{d\mathbf{x}}{dt} = \mathbf{u}, \quad \frac{d\rho}{dt} + \rho\nabla\cdot\mathbf{u} = 0,$$
$$\rho\frac{d\mathbf{u}}{dt} = -\nabla p - \rho\nabla\mathbf{\Phi}, \tag{1}$$
$$\rho\frac{d\varepsilon}{dt} + p\nabla\cdot\mathbf{u} = 0, \quad \eta = \frac{1}{\rho} = \frac{T\mathcal{R}}{p}, \quad \varepsilon = \frac{T\mathcal{R}}{\gamma - 1},$$
$$\nabla^2\mathbf{\Phi} = 4\pi G\rho.$$

where $\frac{d}{dt}$ is the material time derivative, $\mathbf{x} = (r, z)$, $\mathbf{u} = (u^r, u^\phi, u^z)$ is the velocity vector, p pressure, ε internal energy, $\mathbf{\Phi}$ gravitational potential, ρ density, T temperature, G gravitational constant, $\mathcal{R}$ universal gas constant, and γ adiabatic exponent. Axial and cylindrical symmetry are assumed.

For the initial conditions, we assumed that the cloud is a rigidly rotating uniform gas sphere with the following parameters:

$$\begin{aligned} &\rho = 1.492 \times 10^{-17}\ \mathrm{g/cm^3}, && p = 1.548 \times 10^{-10}\ \mathrm{dyn/cm^2}, \\ &r = 3.81 \times 10^{16}\ \mathrm{cm}, && \omega = 2.008 \times 10^{-12}\ \mathrm{rad/s}, \\ &M = 1.73M_\odot = 3.457 \times 10^{33}\ \mathrm{g}, && \gamma = 5/3, \quad u^r = u^z = 0. \end{aligned} \tag{2}$$

At the outer boundary of the gas cloud, pressure is equal to a small constant ($p = 0.87 \times 10^{-13}$ dyn/cm^2). At the outer boundary of the cloud, gravitational potential $\mathbf{\Phi}$ is defined by an integral formula using the expression for the volume potential.

The set of equations (1) was written in nondimensional form. All dimensional variables were presented in the form $F = F_0\tilde{F}$, where F_0 is the scale factor and $\tilde{F}$ is a dimensionless function. The scale values are chosen as:

$$\begin{aligned} &\rho_0 = 1.492 \times 10^{-17}\ \mathrm{g/cm^3}, && r_0 = z_0 = 3.81 \times 10^{16}\ \mathrm{cm}, \\ &t_0 = 5 \times 10^{11}\ \mathrm{s}, && p_0 = \rho_0 t_0^{-2} r_0^2, \\ &u_0^r = u_0^z = r_0 t_0^{-1}, && \mathbf{\Phi}_0 = 4\pi G\rho_0 r_0^2, \\ &\omega_0 = 1/t_0, \quad T_0 = u_0^2/\mathcal{R}, && \varepsilon_0 = u_0^2. \end{aligned}$$

In terms of the dimensionless variables, the set of equations (1) is written in the form (with tilde omitted):

$$\begin{aligned} \frac{d\mathbf{x}}{dt} &= \mathbf{u}, & \frac{d\rho}{dt} + \rho\nabla\cdot\mathbf{u} = 0, \\ \rho\frac{d\mathbf{u}}{dt} &= -\nabla p - q\rho\nabla\mathbf{\Phi}, & q = 4\pi G\rho_0 t_0^2 \approx 3.127, \end{aligned} \tag{3}$$

$$\rho\frac{d\varepsilon}{dt} + p\nabla\cdot\mathbf{u} = 0, \quad \eta = \frac{1}{\rho} = \frac{T}{\rho}, \quad \varepsilon = \frac{T}{\gamma - 1},$$

$$\nabla^2\Phi = \rho.$$

System (3) is solved with the following boundary conditions:

$$u^z = 0 \text{ at } z = 0;$$

$$u^r = 0 \text{ at } r = 0;$$

at the outer boundary $p = 10^{-6}$ and Φ is defined by the integral formula. Initial conditions in nondimensional variables are the following:

$$\rho = 1, \quad \omega = 1.004, \quad p = 1.78 \times 10^{-3}$$

within the circle $r^2 + z^2 \leq 1$ at $t = 0$.

2 NUMERICAL METHOD AND RESULTS

The numerical method used in our simulation of collapse is based on a first-order implicit conservative Lagrangian scheme on an irregular triangular grid. For further details of the scheme, see Ardeljan *et al.* (1987c) and Ardeljan & Kosmachevskii (1993). It was modified to make it applicable to the case of a rotating gas cloud. Details of this modification and testing will be published elsewhere (Ardeljan *et al.*, 1993).

Initially the cloud has

$$\alpha = E_{\text{in}}/|E_{\text{gr}}| = 0.00425, \; \beta = E_{\text{rot}}/|E_{\text{gr}}| = 0.324,$$

here E_{in} being internal energy, E_{gr} gravitational energy and E_{rot} rotational energy. The parameters α and β lie essentially in the same parameter range where ring was obtained by Boss (1980). At the initial collapse stage, the cloud begins to contract along the z axis rather than along the equatorial plane due to lower pressure and rapid rotation. Influence of the gravitational force is balanced in the r direction by the centrifugal force. It should be noted that at these times a "dumbbell" structure does not appear in the density distribution $\rho(z)$ as it does in simulations of Ardeljan *et al.* (1987a). The origin of that "dumbbell" structure is numerical error in the calculation of the gravitational force.

The velocity field shows that matter falls to the equatorial plane throughout most of the computational domain. Gas moves slowly along the equatorial plane only at periphery. At $t = 1.276856$, the cloud continues to contract and becomes flatter; density at the center of the cloud is $\rho \sim 150\rho_0$. In spite of the fact that an implicit difference scheme is used, the solution of (1) changes with time so rapidly at that stage that, in order not to reduce the accuracy of the calculations, we have chosen the value of the time step corresponding to the Courant number which is less than one (see Richtmyer & Morton, 1967).

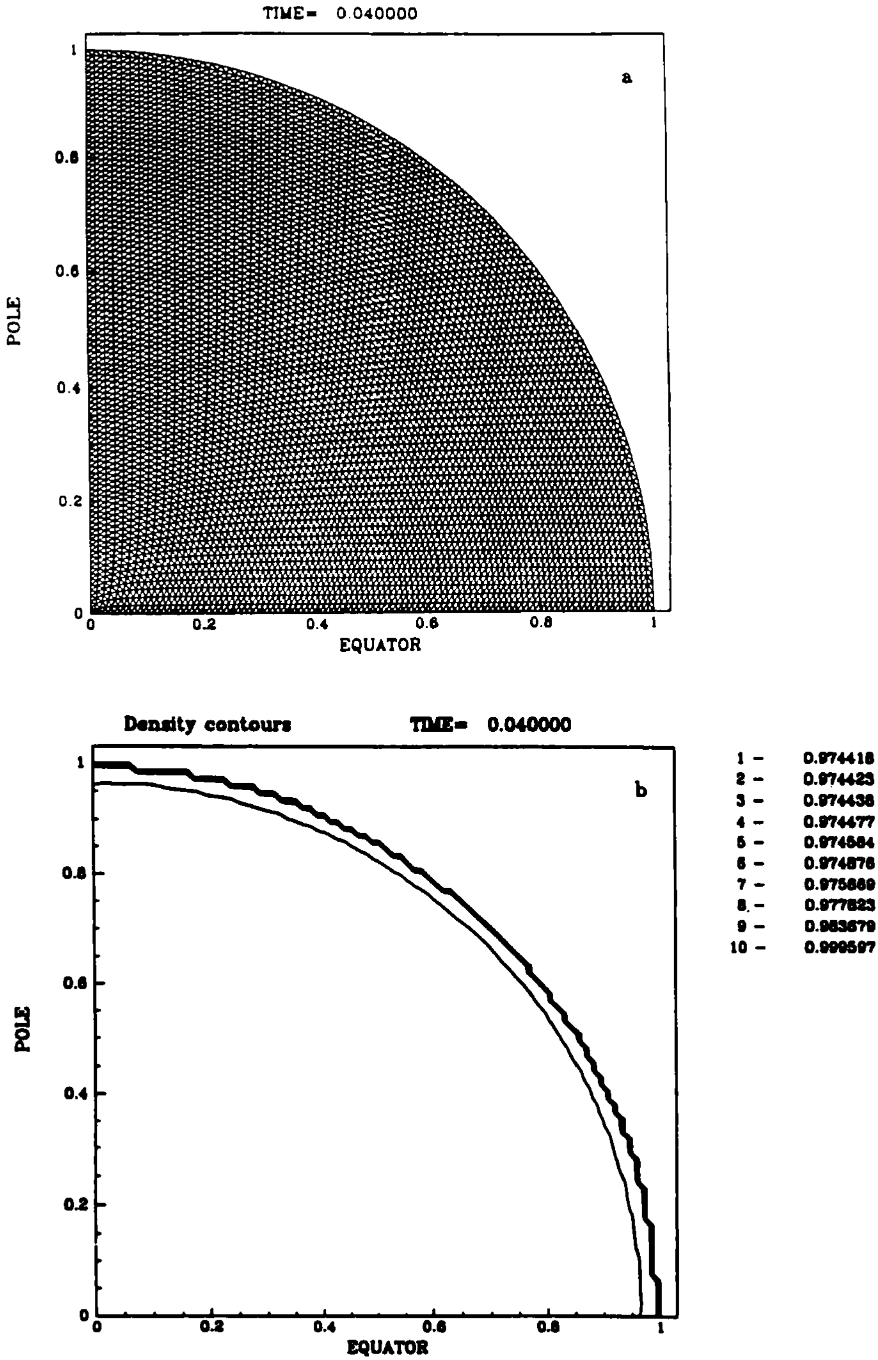

Figure 1 Numerical grid (a) and density contours (b) for $t = 0.040000$.

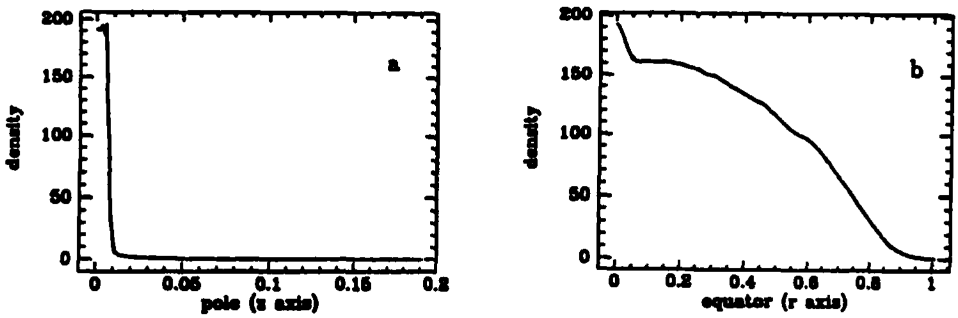

Figure 2 Density distribution along the z-axis (a) and r-axis (b) for $t = 1.285635$.

A time sequence of the cloud shapes is shown in Figure 7. In the inner parts of the cloud density grows monotonically up to the moment $t = 1.285635$ moment of maximum contraction), and, at that moment, it amounts to $\rho \sim 195\rho_0, \rho$ being the initial density here (Figures 2a–b).

Availability of the grid restructuring is important at this stage of calculations. Otherwise, the triangular grid would be distorted due to strong, nonuniform contraction. At the final stage of the first contraction at $t = 1.285635$, the cloud has an ellipsoidal shape with semiaxes in a ratio of $\sim 1 : 5$. The internal part of the cloud, which contains up to 90% of matter, is an ellipsoid with semiaxes in a ratio of $\sim 1 : 100$ (Figure 2a). The number of grid points in every section parallel to the polar axes is no less than 15 at this stage of collapse (the calculated region is a quarter of the ellipse). The cloud contracts up to $t = 1.285635$ when a shock wave appears. Plots for $t = 1.299834$ (Figures 3a–b) show the stage when the shock is definitely formed and reflected at the equatorial plane. The front of the shock can be clearly seen in a plot for the central part of the velocity field (Figure 3b).

Velocity field near the equatorial plane has a quasi-periodic vortex-like structure (see Figure 3b), and a set of feeble rings appears near the equatorial plane. The quasiperiod is about ten knots in the r direction; therefore, we conclude that it is a physical rather than numerical phenomenon resulting from an instability in the gravitational field behind the shock wave.

The wave structure behind the shock in the presence of gravitational force was studied analytically in a 1D acoustical approach by Lamb (1909) and numerically for 1D gravitational gas dynamics by Kosovitchev & Popov (1979). The main reason for this effect is the influence of gravitational field on dispersion properties of matter. Our 2D picture could be induced by the same effect.

The same "wiggly" structure of velocity field was found in calculations of the initial stage of the same collapse problem made using the piece parabolic method on Eulerian grid (Ruffert, 1994).

The formation of the shock wave and its reflection signify the end of the first contraction stage.

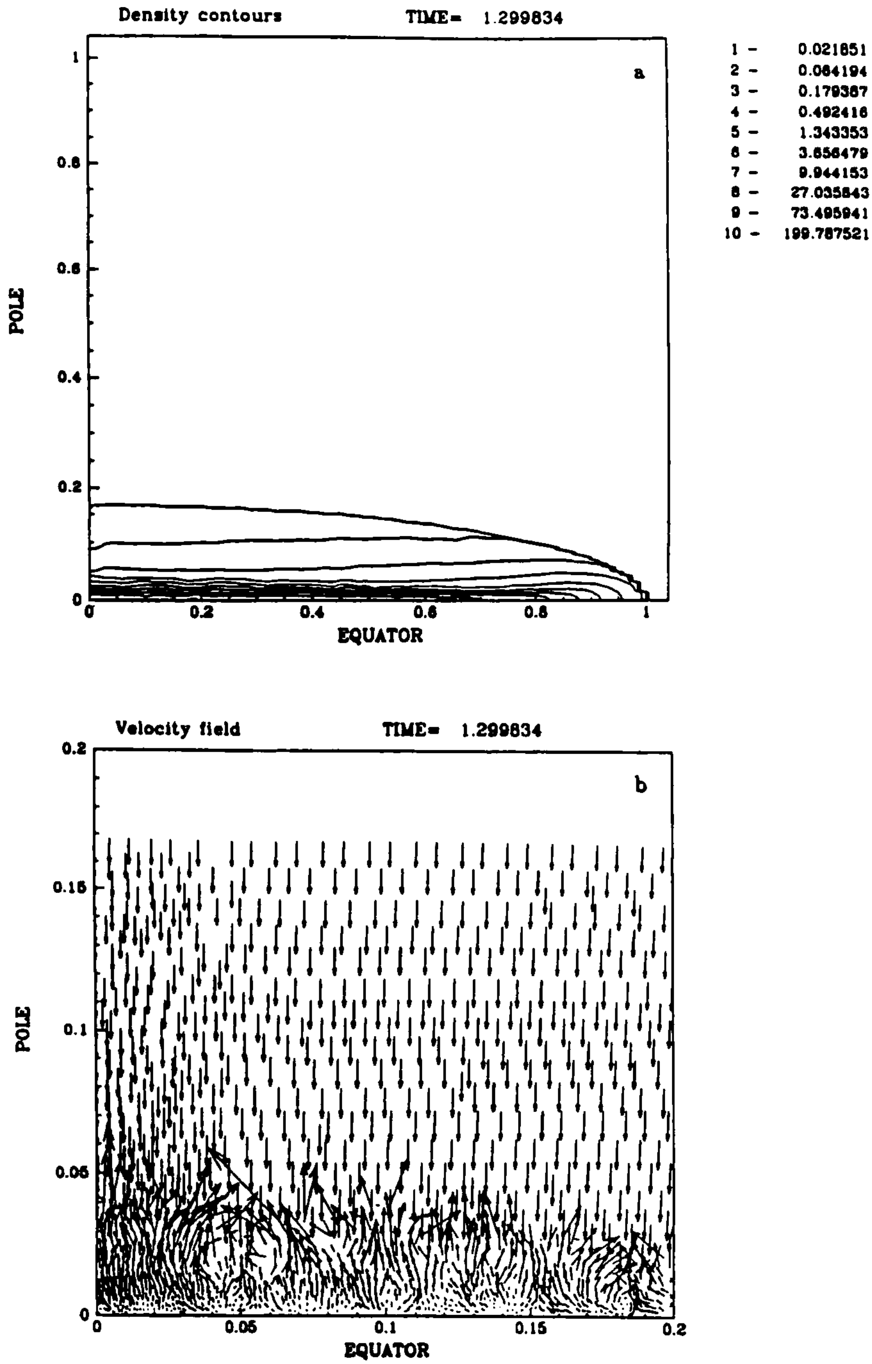

Figure 3 Density contours (a) and central part of the velocity field (b) for $t = 1.299834$.

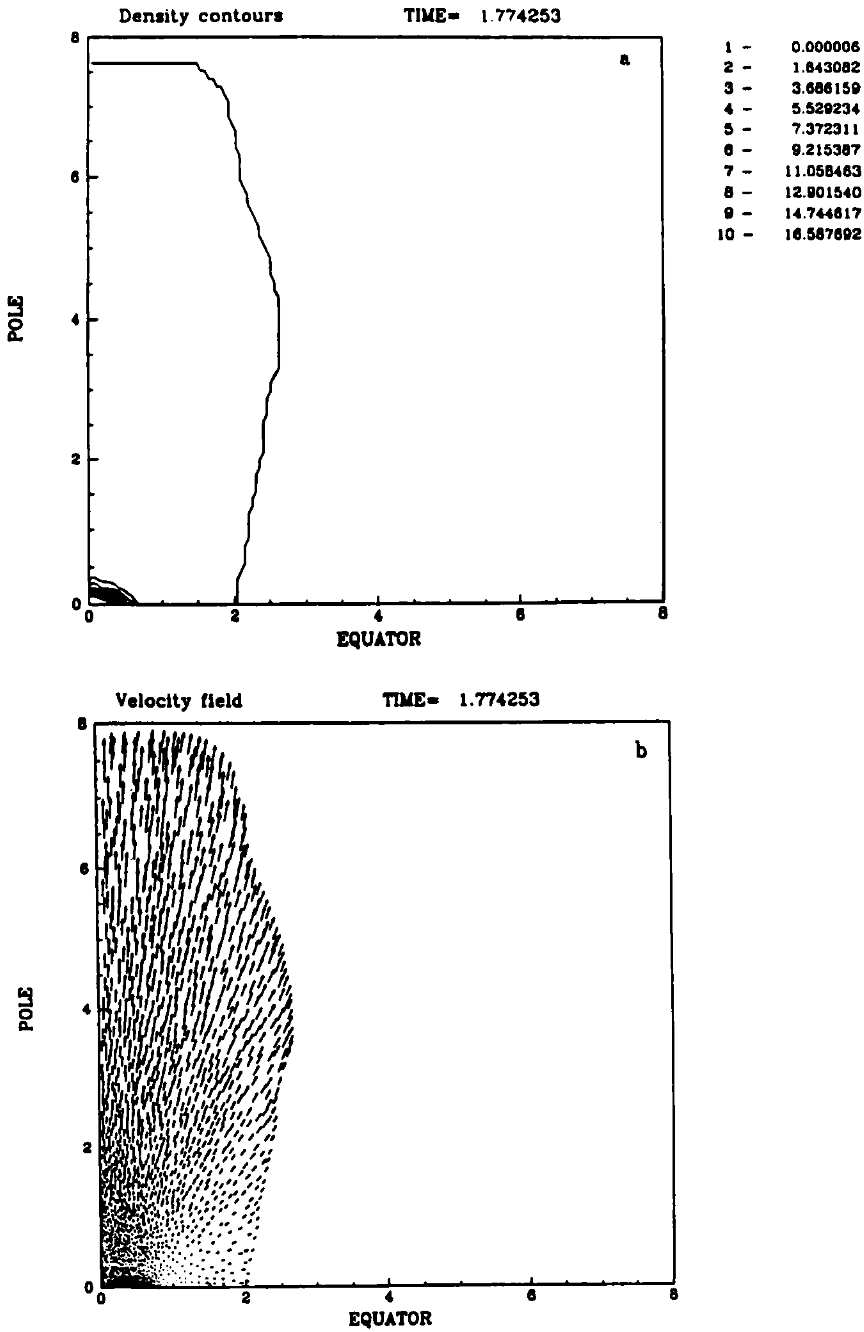

Figure 4 Density contours (a), velocity field (b), central part of the velocity field (c), density distribution along the z-axis (d) and r-axis (e) and distribution of angular velocity along the r-axis (f) for $t = 1.774253$.

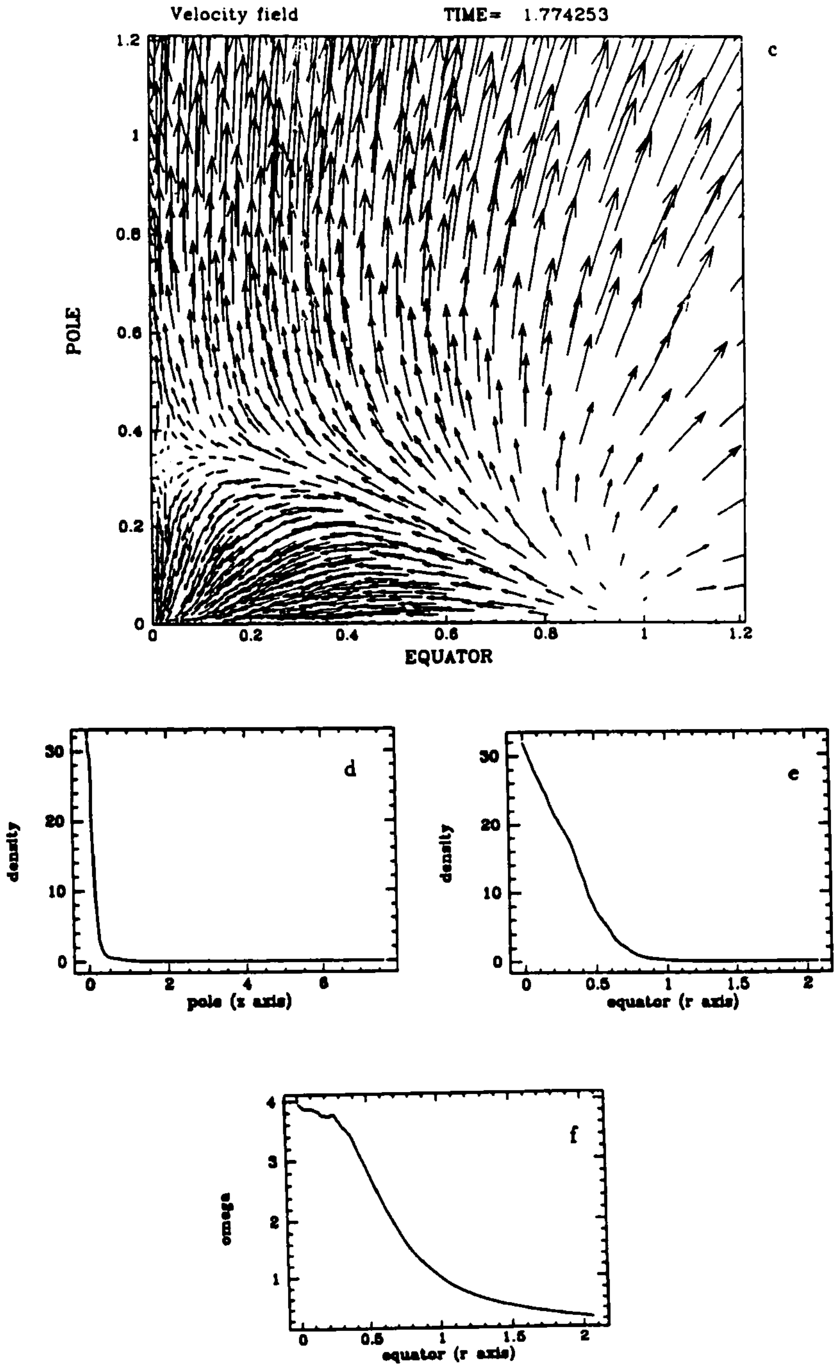

Figure 4 Continued.

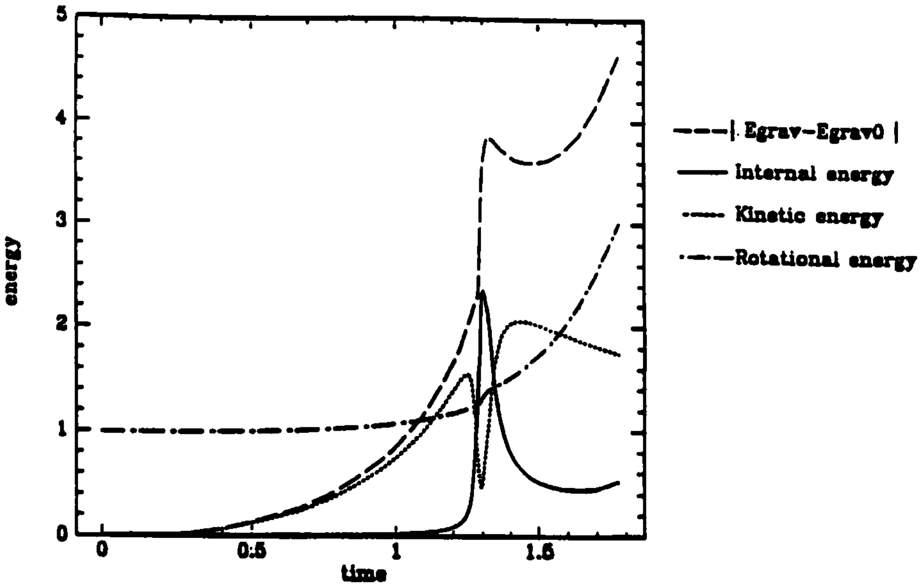

Figure 5 Time variation of different types of energy.

This shock is stronger near the z-axis than in the outer regions and moves faster near the axis of rotation. Behind the front of the shock, density decreases rapidly. The shock wave reaches the outer boundary of the cloud near the z-axis at $t = 1.314921$, with the density in the central cells being $\rho \sim 93\rho_0$. The density distribution $\rho(r)$ has a ring structure along the equator, i.e., the maximum density in the vicinity of the equatorial plane is reached not at the center of the cloud, but in its outer part. At that intermediate stage, density distribution near the plane resembles the final density distribution obtained with Eulerian difference schemes with similar initial conditions (Boss, 1980; Boss, 1989).

At this stage of collapse, the Lagrangian and the Eulerian approaches give qualitatively similar results (i.e., a ring-like density distribution). After shock formation, gas velocity near the equatorial plane changes its sign due to reflection. Although matter expands in the inner parts of the cloud behind the shock, the light envelope continues to contract until the shock reaches the free boundary of the cloud at $t = 1.314921$. The Mach number, characterizing the strength of the shock, is $M \approx 30$ near the center of the cloud soon after the moment of maximum contraction and the shock wave reflection. The shock amplifies (and the Mach number increases) while it propagates outside the cloud.

Instability appears later at the contact point of the shock wave and the free boundary. This leads to the overturning of the part of the envelope near the z-axis. This effect has no significant influence on the processes occurring in the core of the cloud, but it precludes running our code further owing to the nonlocal overlapping of the grid. To avoid this difficulty and to reduce curvature in the free boundary,

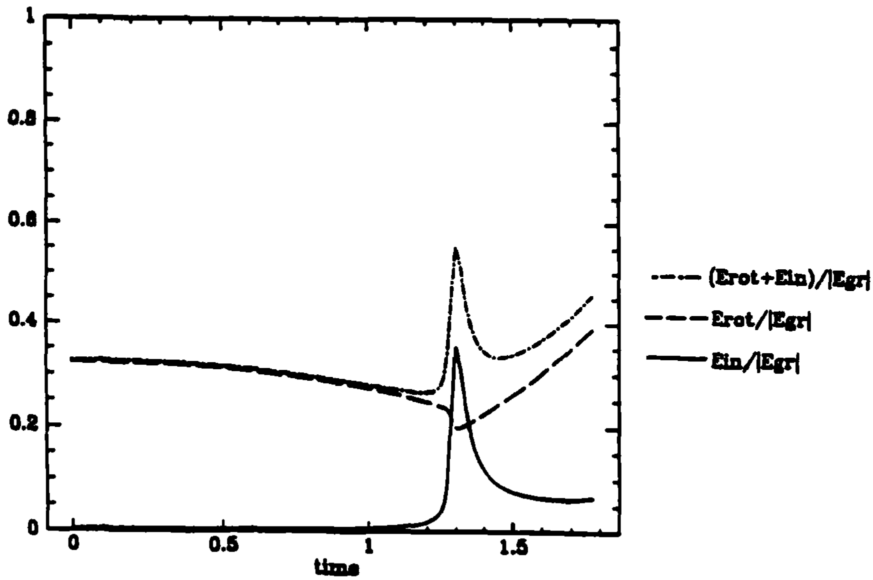

Figure 6 Time variation of $\alpha = E_{in}/|E_{gr}|, \beta = E_{rot}/|E_{gr}|$ and $\alpha + \beta$.

velocities in the boundary mesh points were altered slightly by introducing a special operator in the difference scheme.

The maximum density is still reached in outer regions on the equatorial plane, and the density distribution has a definite ring-type structure. The cloud begins to blow up and, at $t = 1.356753$, the shape of the cloud is close to its initial one (unit sphere), but with significantly nonuniform density distribution. After that moment the cloud also begins to expand in the radial direction of the equatorial plane. When the contact point of the outer boundary and the shock wave reaches the equatorial plane the shock wave disappears but the cloud continues to blow up and, at $t = 1.404643$, has the shape of an ellipsoid prolate along the z axis. The constant-volume boundary condition, if applied at the outer boundary of the cloud, could at that stage of the collapse lead to a deviation of the flow picture from the real one.

The cloud rotates almost rigidly during the first contraction and the following expansion stages. Only a small outer part of the envelope near the r axis rotates at a lower angular velocity. At $t = 1.499228$ the cloud consists of a small dense core and an envelope extremely stretched in the z direction. At that stage the cloud begins to rotate differentially: central parts (close to the z-axis) rotate faster than outer parts of the cloud. The maximum density is still situated on the periphery of the equatorial plane. After $t = 1.499228$, the maximum density is located at the center of the cloud, and from this moment the density distribution preserves a disk-like structure. The central density of the cloud continues to decrease and reaches its minimum $\rho \sim 10\rho_0$ at $t = 1.499228$.

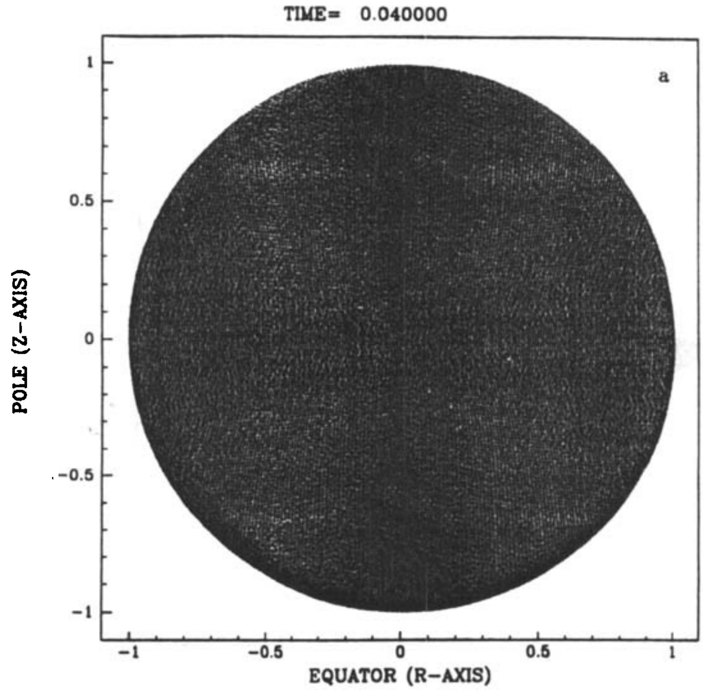

Figure 7 (a–c). Time evolution of the shape of the cloud.

The second contraction starts in the core of the cloud after $t = 1.499228$. The density slowly grows at the center. A low-mass, extended envelope continues to expand, part of its matter ($\sim$ 5%) has kinetic energy larger than its potential energy and moves away to infinity from the cloud. The calculations ended at $t = 1.774253$. The maximum relative error for the total energy was 4.9% at the end of the calculations.

Figure 5 presents time variation of different types of energy. Figure 6 shows time variation of $\alpha = E_{\rm in}/|E_{\rm gr}|$, $\beta = E_{\rm rot}/|E_{\rm gr}|$ and $\alpha + \beta$. The second contraction begins after $t = 1.499228$ with

$$\alpha \approx 0.08, \ \beta \approx 0.34, \tag{4}$$

(see Figure 6). In the collapse simulations of Boss (1980), based on an Eulerian difference scheme, the disk was obtained with initial parameters close to (4). We conclude that the second and all following contractions definitely lead to the formation of a disk-shaped figure.

Acknowledgements

The authors would like to thank Max Plank Institute of Astrophysics in Garching for providing us good computer facilities and hospitality. G. S. B.-K. and S. G. M.

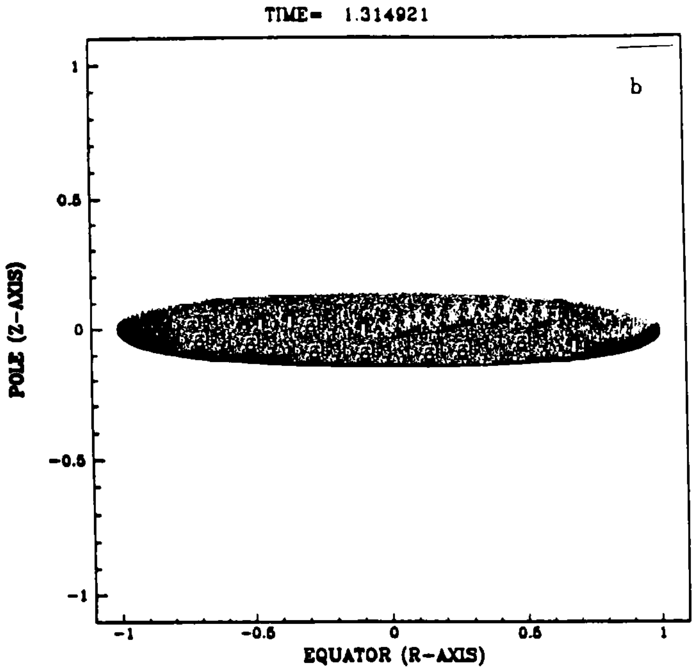

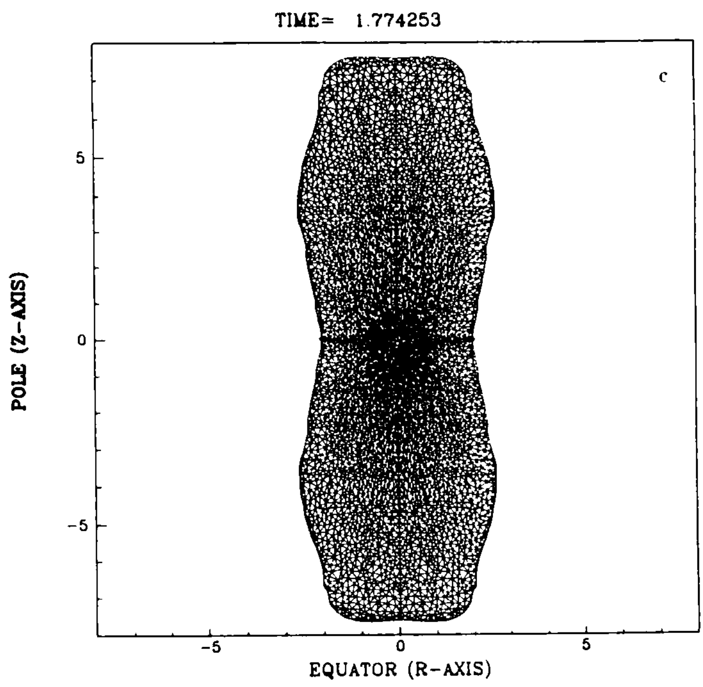

Figure 7 Continued.

were supported partly by the International Science Foundation grant No. M34000, Russian Foundation of Fundamental Researches grant No. 93–02–17106 and Russian Ministry of Science Astronomy Program No. 3–169.

References

Ardeljan, N. V. and Chernigovskii, S. V. (1984) *Differents. Uravneniya* **20**, 1119.

Ardeljan, N. V. and Kosmachevskii, K. V. (1993) *Preprint MPA (Garching)* No. 716.

Ardeljan, N. V., Kosmachevskii, K. V., and Chuvashev, S. N. (1985) *Proc. 11th International Conference on Problems of Methematical Simulation, Programming and Mathematical Methods in Physical Problems*, Dubna, OIJAI, p. 216.

Ardeljan, N. V., Bisnovatyi–Kogan, G. S., Kosmachevskii, K. V., and Moiseenko, S. G. (1993) *Preprint MPA (Garching)* No. 715.

Ardeljan, N. V., Bisnovatyi–Kogan, G. S., Popov, Yu. P, and Chernigovskii, S. V. (1987a) *Astron. Zh.* **64**, 495 [*Sov. Astron.* **31**, 261, 1987].

Ardeljan, N. V., Bisnovatyi–Kogan, G. S., Popov, Yu. P., and Chernigovskii, S. V. (1987b) *Astron. Zh.* **64**, 761 [*Sov. Astron.* **31**,398, 1987].

Ardeljan, N. V., Kosmachevskii, K. V., and Chernigovskii, S. V. (1987c) *Problems of Construction and Analysis of Conservative Difference Scheme for Magnetogas Dynamics*, Moscow (in Russian).

Bisnovatyi–Kogan, G. S. (1970) *Astron. Zh.* **47**, 813 [*Sov. Astron.* **14**, 652, 1971].

Boss, A. P. (1980) *Ap. J.* **242**, 699.

Boss, A. P. (1989) *Private communication.*

Black, D. C. and Bodenheimer, P. (1976) *Ap. J.* **206**, 138.

Bodenheimer, P. and Tscharnuter, W. (1979) *A&A* **74**, 288.

Chandrasekhar, S. (1973) *Ellipsoidal Figures of Equilibrium*, New Hawen.

Kamiya, Y. (1977) *Progr. Theor. Phys.* **58**, 802.

Kosovitschev, A. G. and Popov, Ju. P. (1979) *Journ. Math. Phys. Comp. Math* **19**, 1251.

Lamb, H. (1909) *Proc. London Math. Soc.* **7**, 122.

Larson, R. B. (1972) *MNRAS* **156**, 437.

Miyama, M. (1992) *PASJ* **44**, 193.

Norman, M. L., Wilson, J. R., and Barton, R. T. (1980) *Ap. J.* **239**, 968.

Ostriker, J. P. and Peebles, P. J. E. (1973) *Ap. J.* **186**, 467.

Richtmyer, R. and Morton, K. (1967) *Difference Methods for Initial-Value Problems*, New York.

Ruffert, M. (1994) *Private communication.*